Infrared Physics & Technology 130 (2023) 104607

Contents lists available at ScienceDirect

Infrared Physics and Technology

journal homepage: www.elsevier.com/locate/infrared

Radiometric calibration algorithm for high dynamic range infrared imaging system

Guoqing Yang [a], Yi Yu [a,*], Zhiyuan Sun [a], Zhou Li [a], Xinyu Pang [a,b], Tao Zhang [a]

[a] Changchun Institute of Optics, Fine Mechanics and Physics, Chinese Academy of Sciences, Changchun 130033, China
[b] University of Chinese Academy of Sciences, Beijing 100049, China

ARTICLE INFO

Keywords:
Radiometric calibration
High dynamic range imaging
Radiometry
Infrared radiation transmission and conversion

ABSTRACT

The infrared imaging system with high dynamic range is one of the most prime candidates in the area of quantitative infrared radiometry and thermometry applications. As the foundation of the measurement processes, radiometric calibration is the inception procedure which will be studied emphatically in this paper. Conventional radiometric calibration algorithm is not suitable for high dynamic range infrared imaging systems that requires the flexibility of adjusting the integration time and transmittance according to characteristics of the detected target. Unfortunately, fixed calibration coefficients will inevitably arouse the deterioration of the calibration accuracy in the case of variable integration time or the transmittance. For the purpose of solving above issues, effects of integration time and transmittance on calibration are analyzed in detail. A modified calibration algorithm considering the integration time and transmittance is proposed to compensate the calibration error caused by the change of these two factors. Experiments confirm that the accuracy of the proposed calibration algorithm can reach about 1 % under the conditions of varying integration time and transmittance, which is effectively applicable to high dynamic range infrared imaging applications.

1. Introduction

Radiometric calibration, the critical procedure in quantitative measurement of infrared radiometry or thermometry, intends to obtain calibration coefficients for inverse calculations of radiation or temperature properties of the targets [1–4]. Conventional radiometric calibration strategy is to quantificat the linear-relationship between blackbody radiance and image gray level under a specified integration time, which would be confronted with the issue of inevitably reduced accuracy of the calibration due to the fluctuant system integration time or optical transmittance [5,6]. With the increasing demand of engineering applications, the function of high dynamic range imaging (HDRI) of infrared imaging system is emphasized beyond the basic function of quantitative infrared-image-processing. In engineering applications, the high dynamic range among mid-wave infrared is generally greater than 45 dB, which means that it has the capability to detect both low temperature targets in space and high temperature targets such as exhaust flame. A feasible method is presetting multiple integration times of the camera, as well as adding multiple optical filters with various transmittance, for the purpose of increasing the detectable range of the system without overexposure of the image. The limitation of conventional radiation calibration method is laid bare by this phenomenon. The extracted calibration coefficients should be updated whenever the integration time or optical transmittance of the system is switched. The calibration formula, which is able to reflect the specific linear- relationship, can be thus established according to various integration time and optical transmittance. Therefore, this paper puts forth effort to investigate a new radiometric calibration algorithm which can adapt to the switching of the integration time and optical transmittance.

The linear-relationship between the output image gray level of the detector and its integration time has been described in EMVA Standard 1288 [7]. The absorbed photons energy in the quantum well of the quantum detector increases linearly with the integration time, which is directly reflected in the detector output gray level. M. Ochs proposes a pixel calibration method based on the integration time to achieve high dynamic range calibration with considerable calibration accuracy [8]. S. Chang proposes a calibration algorithm considering the integration time and ambient temperature variation, which is extremely suitable for the conditions of ambient temperature variation in the external field [9,10]. However, the effects of the change of the system filter transmittance are still remained unresolved in above researches. Switching system transmittance, equivalent to the replacement of a lens in the system optical

* Corresponding author.
E-mail address: 13756006195@139.com (Y. Yu).

https://doi.org/10.1016/j.infrared.2023.104607
Received 29 October 2022; Received in revised form 8 February 2023; Accepted 13 February 2023
Available online 23 February 2023

path, will not only change the amount of radiation of the filter itself, the stray radiation will be influenced as well. Stray radiation is caused by the own-radiation and reflection of the lens whose temperature exceeds 0 K, lens baffle and mechanical mechanism which can be calculated and analyses by Codev or Zemax [11–13]. Z. Sun considered the influence of filter transmittance and integration time when calibrating the with large-aperture and wide-dynamic-range infrared system, and proposed the corresponding calibration formula [14]. However, the reflected radiation caused by the filter is remained unconsidered, in other words, a corresponding calibration coefficient is missing. In brief, investigating new strategy of increasing the integration time and transmittance-dependent radiation calibration accuracy is an urgent but unresolved issue in infrared radiometry. These two factors on the impact of radiometric calibration have yet to be further in-depth study.

In this paper, the influence of two factors, integration time and filter transmittance, on radiometric calibration is further investigated in detail. A new calibration formula is derived, which contains three variables including integration time, transmittance and incident radiance. Two more variables are introduced compared to the traditional calibration formula to achieve high dynamic range calibration. Finally, a new calibration algorithm is proposed to solve the coefficients in the calibration equation.

2. Principle of radiometric calibration algorithm

2.1. Traditional calibration algorithm

Conventional calibration algorithms generally focus on two main routes: absolute calibration and relative calibration. Absolute calibration aims at obtaining the relationship between the incident radiance and the output image gray level, which is the most elementary process for the target radiometry or thermometry system [15]. Relative calibration, essential procedure in high imaging quality requirements situation, refers to the non-uniform correction algorithm which is capable of correcting the detector image photon responsiveness inconsistency or correcting the fixed bad points. For the high imaging quality requirements of the system this is also a necessary step. This paper mainly focuses on the absolute calibration algorithm.

For small-aperture infrared imaging systems, the most frequently-used calibration method is external-surface-source-calibration (ESSC) strategy [1,6,16,17], as shown in Fig. 1. In ESSC strategy, a uniform source with known radiance is placed before the pupil, which can fill the entire field of view (FOV), for the purpose of adjusting the incident radiation and obtaining the output image gray level. The calibration response parameters of the system can be extracted according to the linear-relationship between a series of input radiation and output gray level, so as to complete the calibration operation.

Blackbody is the most commonly-used uniform radiation source, of which the emissivity is close to 1 [18]. According to Planck's law of radiation, the incident radiance $L(T_b)$ of the blackbody can be accurately calculated at the specified temperature, as shown in Eq. (1).

$$L(T_b) = \varepsilon \cdot \int_{\lambda_1}^{\lambda_2} L_\lambda(T_b) d\lambda = \varepsilon \cdot \int_{\lambda_1}^{\lambda_2} \frac{c_1}{\pi \cdot \lambda^5 (e^{c_2/\lambda T_b} - 1)} d\lambda \tag{1}$$

where ε is the emissivity of the blackbody radiation source. $L_\lambda(T_b)$ denotes the spectral radiance of an ideal blackbody at a temperature of T_b. λ_1 and λ_2 are the spectral limits of detection. c_1 and c_2 are the first and the second radiation constants, respectively. $c_1 = 3.7415 \times 10^8$ W·μm^4·m^{-2} and $c_2 = 1.4388 \times 10^4$ μm·K.

Relationship between the output image gray level of the detector and incident radiance can be approximatively expressed by a linear-relationship, as shown in Eq. (2).

$$g_{i,j} = G_{i,j} \cdot L(T_b) + O_{i,j} \tag{2}$$

where $g_{i,j}$ is the gray value [digital number (DN)] at (i, j) in the infrared focal plane array (IRFPA). $G_{i,j}$ and $O_{i,j}$ are the response gain and offset values of the imaging system, respectively. In practical engineering applications, more than two sets of data are generally collected and the calibration parameters can be calculated by using the least-square-fitting method.

For high dynamic range infrared radiometry system, multiple integration time and filters should be set. The output gray level of infrared detector is related to the integration time which affects the incident radiation energy. Therefore, the calibration formula is dependent on the integration time. In addition, the introduced filter reduces the incident radiation on the infrared detector, however the infrared radiation and reflected radiation of the filter itself increase the stray radiation entering the infrared detector. Therefore, the calibration formula is also dependent on the transmittance controlled by the filter. The calibration parameters should be updated appropriately along with the switching of integration time or the filter.

2.2. Radiometric calibration accuracy evaluation

The accuracy of the radiometric calibration is a criterion to assess the quality of the calibration algorithms. Generally, radiometric calibration is a reciprocal process towards the radiometry or thermometry process, therefore, the calibration accuracy should also be derived from the principle of radiometry [19]. Once the system is calibrated, calibration coefficients $G_{i,j}$ and $O_{i,j}$ can be obtained. If the gray level of the target image is known, the radiance of the target can be calculated based on the extracted gray level according to the derivation of Eq. (2). The device of the ESSC strategy in Fig. 1 is also applicable to the evaluation of the radiometric calibration accuracy. Assuming that the blackbody temperature is T_b, its true radiance is $L(T_b)$, and the obtained output image gray value is g', then the radiance $L'(T_b)$ obtained by the calibration inversion can be calculated according to Eq. (2).

$$L'(T_b) = \frac{g'_{i,j} - O_{i,j}}{G_{i,j}} \tag{3}$$

Therefore, the radiometric calibration error can be expressed as.

$$error = \frac{L'(T_b) - L(T_b)}{L(T_b)} \times 100\% \tag{4}$$

For high-accuracy radiometry or thermometry, the error should be within 5 % or even lower. The error is mainly related to the factors including temperature accuracy and stability of the referenced blackbody, the performance of the detector and the ambient temperature stability.

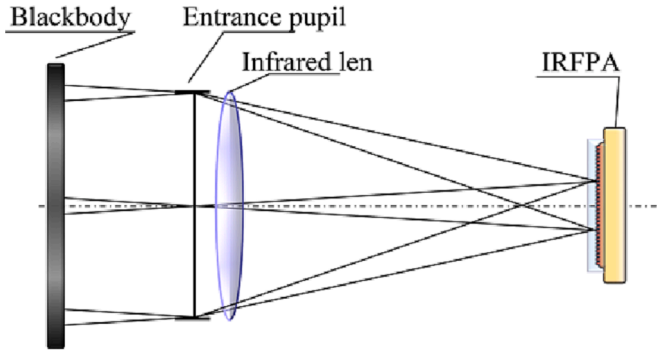

Fig. 1. Schematic diagram of ESSC strategy.

2.3. The effect of integration time and transmittance on calibration

For the purpose of analyzing the effect of integration time and transmittance on radiometric calibration, the principle of radiometry should be emphatically concerned. Radiation entering the infrared system can be transmitted by the optical system and extracted by the detector, which is then converted into electrical signals. Therefore, we will focus on the radiation transmission and conversion processes in the following discussion.

Assuming that a uniform radiation enters the pupil of an optical system and passes through the optical system and then enters the IRFPA, the received radiation flux on a single pixel can be expressed as follows [9]:

$$\Phi = \frac{\pi \cdot \tau_{opt} \cdot A_d \cdot D^2 \cdot \cos\theta^4}{4f^2} \cdot L(\lambda) = G_1 \cdot L(\lambda) \tag{5}$$

where, D is the aperture of the pupil, A_d is the area of per pixel of the IRFPA, τ_{opt} and f are the transmittance and focal length of the optical system, respectively, $L(\lambda)$ is the incident uniform radiance with the wavelength of λ on the entrance pupil of the optical system. For ground-based infrared optical system, the FOV is in the range of a few degrees, that is, cos $\theta \approx 1$. G_1 can be regarded as a parameter independent of incident radiation. In conclusion, the relationship between the radiation flux Φ received by a single pixel and the incident radiance $L(\lambda)$ can be fitted as a linear-correlation.

Photons received by a single pixel are converted into electrical signal through a photo-electric conversion process. Then, after signal processing, the output gray value of the digital image can be obtained. The above process can be described:

$$g = \frac{K \cdot \eta(\lambda) \cdot \Phi \cdot t \cdot \lambda}{h \cdot c} + g_d = G_2 \cdot \Phi + g_d \tag{6}$$

where Φ is the radiation flux with the specific wavelength λ received by a single pixel in the integration time t, h is the Planck constant and c is the speed of light. Quantum conversion efficiency $\eta(\lambda)$ is defined as the ratio of the number of charges generated by light excitation to the number of incident photons on the photosensitive material, which is related to wavelength λ. K is the global linear gain of the detector. The dark field signal g_d is the obtained gray value in the absence of incident radiation.

According to Eq. (5) and (6), the relationship between the output gray level of the pixel and the incident radiance at the entrance pupil can be obtained as follows:

$$g = G_2 \cdot G_1 \cdot L(\lambda) + g_d = G \cdot L(\lambda) + g_d \tag{7}$$

The form of Eq. (7) is consistent with that of Eq. (2). According to Eqs. (5) - (7), the gain coefficient G of system calibration is not only related to the intrinsic characteristic coefficients of the optical system and the detector, such as focal length and quantum efficiency, but also has a linear-relationship with the integration time of the camera and the transmittance of the filter in the optical system.

The offset O is not only related to g_d in Eq. (7), but also related to the stray radiation of the surrounding environment reflected by the lenses of the system and the internal-generated radiation of the system. Stray radiation and internal-generated radiation will enter the detector, so that the integration time contributes to the offset O aroused from stray radiation and internal-generated radiation. The internal factor of the detector is caused by its own dark signal, which is equal to the obtained gray level without incident radiation, so it is independent of the integration time. Therefore, the offset O can be expressed as.

$$O = t \cdot g_{out} + g_{in} \tag{8}$$

g_{out} is the gray value caused by stray radiation and internal-generated radiation, and g_{in} is the gray value caused by the dark signal.

In addition, the self-generated radiation of reflection filters with various transmittances is generally very small. However, the produced reflected radiation is not a negligible factor. The self-generated radiation of the filter is related to its own temperature and emissivity, which will enter the detector directly along with the optical path or be reflected into the detector. The reflected radiation of the filter is related to its own reflectivity, whose energy will be reflected into the detector by the lens, lens baffles and mechanical structures for many times. Propagation process of the filter-introduced radiation is shown in Fig. 2.

It is assumed that the filter temperature is consistent with the ambient temperature of the measuring system under various transmittance. Changes of self-generated radiation caused by switching different filters are extremely small due to their emissivity. Therefore, the gray level introduced by self-generated radiation can be ignored. Reflectance of filters ρ_{ndf} can be expressed as $\rho_{ndf} = 1\text{-}\tau_{ndf}$, so that the gray value offset g_{ndf} caused by filter switching is.

$$g_{ndf} = t \cdot G_{ndf} \cdot (\rho_{sys} \cdot \rho_{ndf} \cdot L_t) = t \cdot G_{ndf} \cdot (1 - \tau_{ndf}) \cdot \rho_{sys} \cdot L_t \tag{9}$$

where L_t is the incident radiance. t is the detector integration time. ρ_{sys} is the reflection coefficient of the elements in the system except for the filter, which is a constant. And G_{ndf} is the gain coefficient of the detector's response to reflected radiation introduced by the filter. Defining that $g_f = G_{ndf} \cdot \rho_{sys} \cdot L_t$, Eq. (9) can be simplified as.

$$g_{ndf} = t \cdot (1 - \tau_{ndf}) \cdot g_f \tag{10}$$

It can be found from Eqs. (8) and (10) that the offset coefficient O of the system is related to both the detector integration time and the filter transmittance.

2.4. Principle of the proposed algorithm

On account of the above analysis, an infrared radiometric calibration algorithm with high dynamic range considering integration time and transmittance is proposed. Assuming that the integration time of the detector is t, the filter transmittance is τ_{ndf}, the radiometric calibration model can be expressed as:

$$g(t, \tau_{ndf}, T_b) = t \cdot \tau_{ndf} \cdot G \cdot L(T_b) + t \cdot (1 - \tau_{ndf}) \cdot g_f + t \cdot \tau_{ndf} \cdot g_{out} + g_{in} \tag{11}$$

There are four unknown quantities in the proposed calibration model, including the response gain G per unit time, gray value offset g_f caused by filter, gray value offset g_{out} caused by external factors such as stray radiation, and gray value offset g_{in} caused by internal factors such as dark current of the detector. To simplify the description, the calibration formula can be written as.

$$f(x, y, z) = G \cdot xyz + g_f \cdot x(1 - y) + g_{out} \cdot xy + g_{in} \tag{12}$$

where

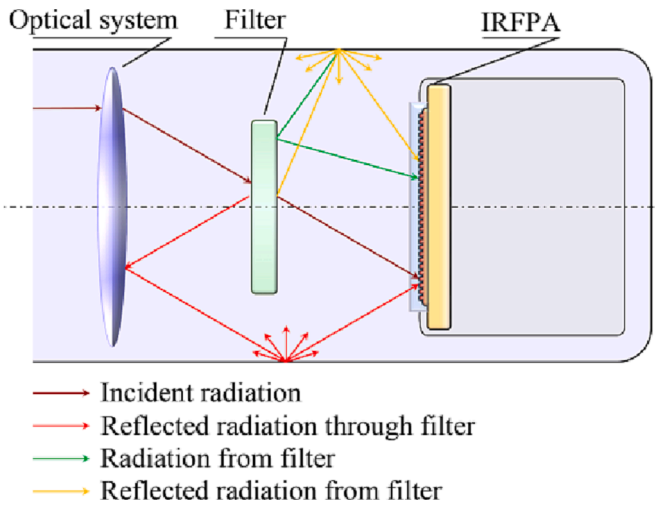

Fig. 2. Radiation propagation process through the filter.

$$\begin{cases} x = t \\ y = \tau_{ndf} \\ z = L(T_b) \\ f(x, y, z) = g(t, \tau_{ndf}, T_b) \end{cases} \tag{13}$$

Residuals can be calculated as.

$$\varepsilon i = G{\cdot}x_i y_i z_i + g_f{\cdot}x_i(1 - y_i) + g_{out}{\cdot}x_i y_i + g_{in} - f(x_i, y_i, z_i) \tag{14}$$

Based on the principle of least squares, gain G and offset g_f, g_{out}, g_{in} can be calculated by solving the equation as follows:

$$\begin{bmatrix} x_1y_1z_1 & x_1(1-y_1) & x_1y_1 & 1 \\ x_2y_2z_2 & x_2(1-y_2) & x_2y_2 & 1 \\ \vdots & \vdots & \vdots & \vdots \\ x_ny_nz_n & x_n(1-y_n) & x_ny_n & 1 \end{bmatrix} \begin{bmatrix} G \\ g_f \\ g_{out} \\ g_{in} \end{bmatrix} = \begin{bmatrix} f_1 \\ f_2 \\ \vdots \\ f_n \end{bmatrix} \tag{15}$$

Four images at different integration time, transmittances and blackbody temperatures are demanded to obtain above calibration parameters. Moreover, the gray level of the collected images should not be saturated to maintain the linear response model. The calibration formula of any integration time and any transmittance can be obtained by substituting the solved calibration parameters into Eq. (11).

3. Experiments and measurement results

The radiometric calibration experiment was implemented to demonstrate the feasibility of the proposed calibration algorithm as shown in Fig. 3. The infrared imaging system consists of a cooled mid-wave infrared camera and an infrared optics system. The camera model CA600MU-01 manufactured by Beijing Xiaotunpai in China, has an IRFPA with 14-bit output, an imaging response band of 3.7–4.8 μm, a focal plane array of 640 × 512 and the pixel size of 15 μm. The optical system has an aperture of 200 mm and a focal length of 800 mm. In addition, the system is equipped with filter wheel, including the average transmittance of 99 %, 45 %, 17 %, 11 % and 7 % in the response band, which is for the purpose of increasing the dynamic range of the system. Transmittance values are tested and verified to ensure the accuracy. An extended area blackbody, namely SR800N, purchased from Elias CI-System is utilized as the reference, whose emissivity is 0.96 in the 3.7–4.8 μm wave band. The radiation surface size is 254 × 254 mm and the temperature range is set as 0 °C to 150 °C with a temperature accuracy of 0.015 °C.

3.1. The effect of integration time on gray level

The relationship between the image gray level and the integration time can be obtained by setting a fixed blackbody temperature and collecting images at different integration time, as shown in Fig. 4. It can be found that there is an obvious linear relationship between image gray level and integration time.

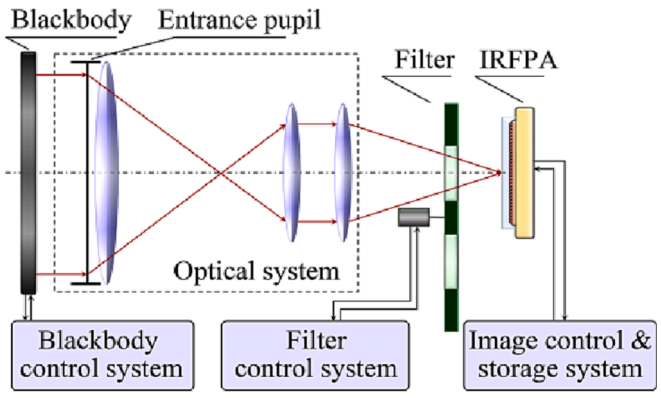

Fig. 3. Diagram of experimental device.

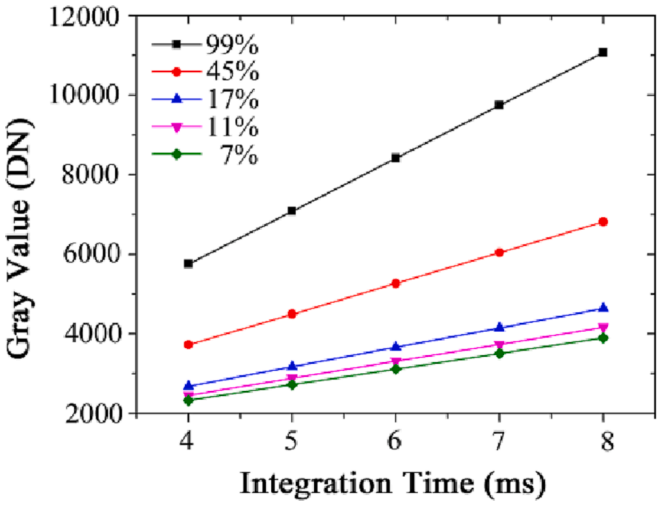

Fig. 4. The relationship between gray value and integration time under various transmittances.

3.2. The effect of filter transmittance on gray level

Meanwhile, the relationship between the image gray level and the transmittance can be obtained by setting a fixed blackbody temperature and collecting images at different filter transmittance, as shown in Fig. 5. It is apparent that, there is an obvious correlation between image gray level and system transmittance.

3.3. The calibration formula obtained through the proposed algorithm

For the purpose of evaluating the accuracy of the proposed calibration algorithm, the formula can be obtained according to the following steps:

(1) The blackbody temperature was set as 50 °C, the integration time was set as 5 ms and 6 ms, and the transmittance of the filter switched to 99 % and 45 %, respectively. Images of the blackbody were collected;
(2) Then, the temperature of the black body was set as 60 °C. Then images of blackbody were acquired with identical integration time and filter transmittance in step (1);

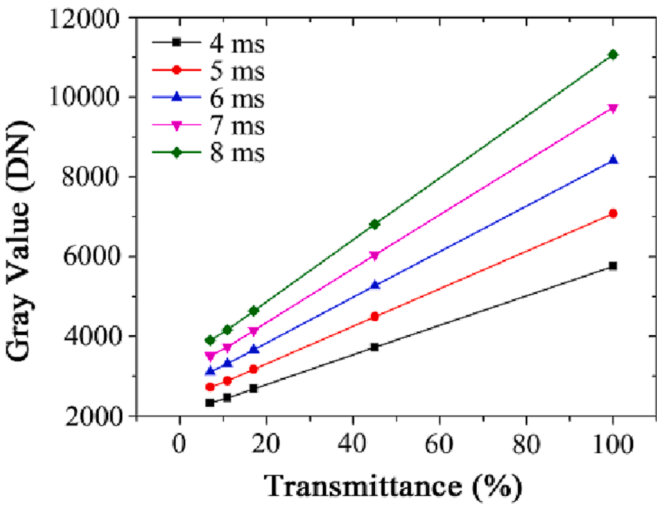

Fig. 5. The relationship between gray value and transmittance at various integration time.

(3) The output gray values of the pixel (320,256) in all images that captured were recorded in Table 1.

On account that the FOV of the optical system is extremely small, such as 1.38°×1.10°, so $\cos\theta^4$ is approximately 1 in Eq. (5). The effect of the FOV on the calibration coefficient can be ignored, which indicates that the proposed calibration algorithm is effective for each pixel.

Substituting the data in Table 1 into Eq. (15), then the calibration coefficient can be obtained through the least square method.

$$\begin{aligned} G &= 292.18 \\ g_f &= 350.84 \\ g_{out} &= 203.19 \\ g_{in} &= 581.26 \end{aligned} \tag{16}$$

Substituting Eq. (11), the calibration formula can be obtained as:

$$\begin{aligned} g(t,\tau_{ndf},T_b) = {} & 292.18t\cdot\tau_{ndf}\cdot L(T_b) + 350.84t\cdot(1-\tau_{ndf}) \\ & +203.19t\cdot\tau_{ndf} + 581.26 \end{aligned} \tag{17}$$

4. Error analysis and discussion

For the purpose of evaluating the calibration accuracy of the proposed algorithm, more blackbody images at different temperatures were obtained at various integration time and transmittances. The integration time of the detector was set from 4 ms to 8 ms, with an interval of 1 ms. The transmittances of filters were set as 99 %, 45 %, 17 %, 11 %, and 7 %, respectively. The temperature of the blackbody was set from 40 °C to 80 °C with an interval of 10 °C.

Firstly, the influence of switching transmittance or integration time on the radiometric calibration accuracy is analyzed. Afterwards, the compensation ability of the proposed calibration algorithm for the accuracy reduction is evaluated. Finally, the calibration accuracy utilizing conventional algorithm at a specific integration time and different transmittances is calculated by the calibration equation as control.

4.1. The effect of switching transmittance and integration time on the radiometric calibration accuracy

The radiometric calibration formula utilizing conventional calibration algorithm with integration time of 6 ms and transmittance of 45 %, respectively, is shown as follows:

$$g(T_b) = 821.67\cdot L(T_b) + 2187.37 \tag{18}$$

In order to evaluate the influence of switching transmittance on the radiometric calibration accuracy, blackbody images at 60 °C with integration time of 6 ms under various transmittances are collected. The obtained gray values are plugged into Eq. (18) to obtain the inverse radiance values. The standard radiance at 60 °C can be calculated as 3.7627 $W\cdot m^{-2}\cdot sr^{-1}$ by Eq. (1) as a reference. According to Eq. (4), the calculated radiometric calibration errors under various transmittances are shown in Fig. 6.

The formula of conventional radiometric calibration algorithm is obtained at the transmittance of 45 %, of which the calibration error is minimal. However, the accuracy of the conventional calibration algorithm will drop sharply, once the transmittance deviates from 45 %, and the error even reaches more than 50 %, which is undoubtedly unacceptable. Therefore, in the condition of changing transmittance, the system should be re-calibrated at new transmittance, and the calibration coefficients at original transmittance should not be used. However, for HDRI, especially continuously variable integration time and transmittance systems, continuous switching transmittance calibration is cumbersome and inefficient, and the conventional calibration algorithm is not applicable. A calibration algorithm with compensation function needs to be proposed to optimize the conventional algorithm.

Table 1
The data used to obtain the calibration formula.

Blackbody Temperature/°C	Integration Time/ms	Transmittance/ %	Output Gray Value/DN
50	5	99	5637
50	5	45	3849
50	6	99	6650
50	6	45	4483
60	5	99	7082
60	5	45	4497
60	6	99	8410
60	6	45	5270

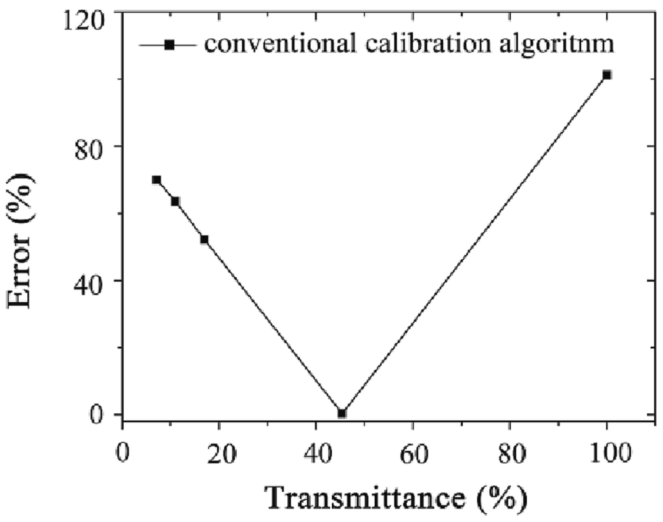

Fig. 6. Error of conventional calibration algorithm under various transmittances utilizing calibration formula at the transmittance of 45 %.

Similarly, the influence of switching integration time on the radiometric calibration accuracy under identical transmittance is shown in Fig. 7. On the grounds that the response of the IRFPA to the integration time is linear thus its error is linear as well. Therefore, the calibration formula solved under a specified integration time cannot be applied to other integration time. Once the integration time changes, the system also needs to be re-calibrated.

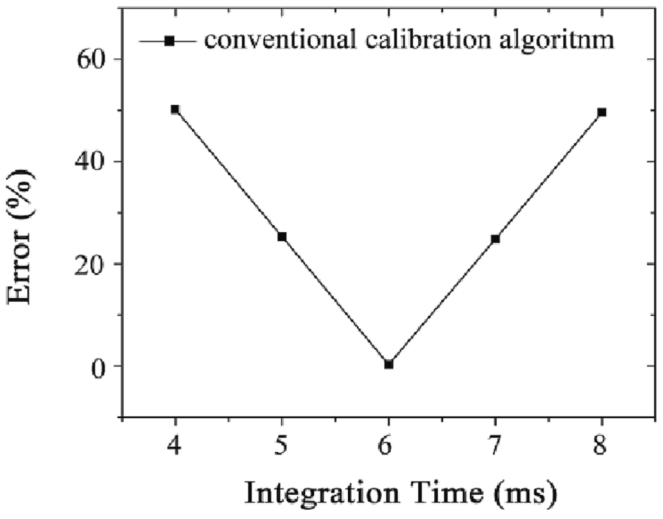

Fig. 7. Error of conventional calibration algorithm under various integration time utilizing calibration formula with integration time of 6 ms.

4.2. Error comparison of the proposed algorithm and conventional algorithm

The radiometric calibration formula utilizing the proposed calibration algorithm under identical conditions can be calculated as follows according to Eq. (17):

$$g(\tau_{ndf}, T_b) = 1753.07\tau_{ndf} \cdot L(T_b) - 885.93\tau_{ndf} + 2686.32 \quad (19)$$

In order to calculate the accuracy of above two radiometric calibration algorithms, the radiometric calibration formula utilizing conventional calibration algorithm with integration time of 6 ms and various transmittances, respectively, is shown Table 2.

The obtained gray values of blackbody images at 60 °C with integration time of 6 ms under various transmittances are plugged into Eq. (19) and calibration formulas of conventional algorithm in Table 2 respectively to obtain the inverse radiance values of the two algorithms. The standard radiance has been calculated as 3.7627 $W \cdot m^{-2} \cdot sr^{-1}$ by Eq. (1) as a reference. According to Eq. (4), the calculated radiometric calibration errors under various transmittances are shown in Fig. 8.

The calibration accuracy of two radiometric calibration algorithms is roughly the same at any transmittance, as shown in Fig. 8. The proposed calibration algorithm is compatible with multiple transmittances, of which the calibration error is about 1 % at any transmittance. Compared with the conventional algorithm, the proposed algorithm has the advantage of not requiring calibration at each transmittance, which improves the calibration efficiency. Comparing Fig. 6 and Fig. 8it is obvious that the proposed calibration algorithm can effectively compensate the calibration error introduced by the switch of transmittance. In brief, the proposed calibration algorithm can indeed modify the calibration formula as the switch of transmittance.

It is worth noting that at low transmittance, the signal-to-noise ratio of the image decreases distinctly, which leads to decrease calibration accuracy. The calibration error of the infrared radiometry and thermometry system in this paper will rise sharply under the transmittance less than 7 %. Therefore, the algorithm proposed in this paper is not suitable for low transmittance infrared systems. In practice, it is not recommended to image the target at low transmittance on account of the extremely poor image quality.

Similarly, the calibration errors of the two radiometric calibration algorithms at different integration time can be calculated under identical transmittance. Results are shown in Fig. 9. It can be found that the calibration accuracy of the two algorithms is similar. The error of the proposed calibration algorithm is less than 1 % under any integration time, which indicates that the accomplished accuracy is competent with practical application.

5. Conclusion

In this paper, a new radiometric calibration algorithm is proposed on the basis of conventional radiometric calibration algorithm. The integration time of the infrared system and the transmittance of the filter are taken into account to realize high dynamic range calibration. The proposed radiometric calibration algorithm owns advantages of enabling high-accuracy radiometric calibration for the infrared imaging system with continuous transformation integration time and transmittance, which is more efficient compared with conventional radiometric calibration algorithm at multiple integration time and transmittances. The influence of integration time and transmittance on the output gray level of the infrared system is analyzed in this paper. Furthermore, calibration formula in regard to these two parameters are derived. Four parameters in the calibration formula are solved by obtaining the blackbody images at different temperatures under two integration time and two transmittances. A new calibration formula is thus obtained. Finally, radiometric calibration experiment is carried out based on the high dynamic range infrared imaging system to evaluate the effectiveness of the proposed calibration algorithm. In accordance with the analysis of the obtained radiometric data, the accuracy of the proposed algorithm can be obtained about 1 % in linear response range of the detector when the infrared image system integration time is within an adjustable range without over exposure and the filter transmittance is above 7 %.

Table 2
The calibration formula utilizing conventional calibration algorithm.

Integration Time/ms	Transmittance/ %	calibration formula of conventional calibration algorithm
6	99	$g(T_b) = 1833.98 \bullet L(T_b) + 1509.83$
6	45	$g(T_b) = 821.67 \bullet L(T_b) + 2187.37$
6	17	$g(T_b) = 302.84 \bullet L(T_b) + 2529.76$
6	11	$g(T_b) = 188.07 \bullet L(T_b) + 2610.78$
6	7	$g(T_b) = 124.06 \bullet L(T_b) + 2654.84$

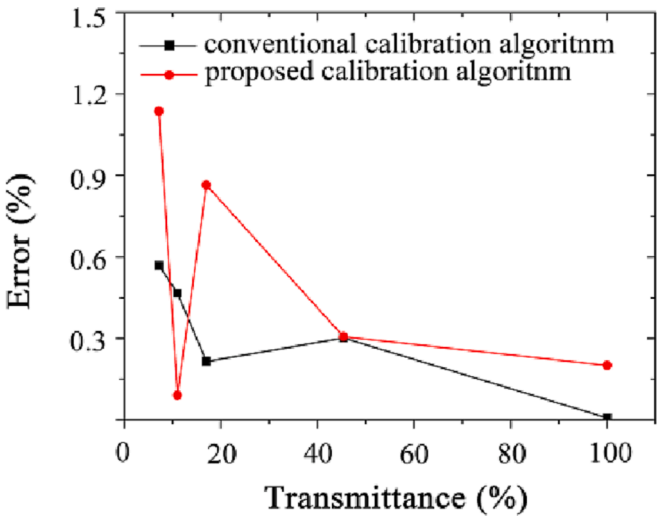

Fig. 8. Error of calibration algorithm under various transmittances.

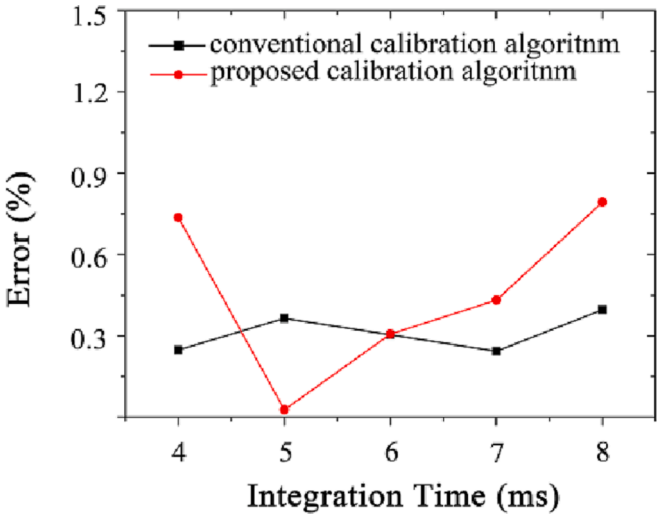

Fig. 9. Error of calibration algorithm at various integration time.

Declaration of Competing Interest

Funding: National Natural Science Foundation of China [6210031610]

Data availability

Data will be made available on request.

References

[1] W. L. Wolfe, *Introduction to radiometry* (SPIE, 1998).
[2] J.M. Palmer, B.G. Grant, *The art of radiometry* (SPIE, 2010).
[3] S. Papini, P. Yafin, I. Klapp, N. Sochen, Joint estimation of unknown radiometric data, gain, and offset from thermal images, Appl. Opt. 57 (2018) 10390–10401.
[4] D.D. Kohler, W.P. Bissett, R.G. Steward, C.O. Davis, New approach for the radiometric calibration of spectral imaging systems, Opt. Express 12 (2004) 2463–2477.
[5] I. Klapp, S. Papini, N. Sochen, Radiometric imaging by double exposure and gain calibration, Appl. Opt. 56 (2017) 5639–5647.
[6] M.D. Mermelstein, K.A. Snail, R.G. Priest, Spectral and radiometric calibration of midwave and longwave infrared cameras, Opt. Eng. 39 (2000) 347–352.
[7] E. M. V. Association, "Standard for characterization of image sensors and cameras," EMVA Standard **1288**(2010).
[8] M. Ochs, A. Schulz, H.-J. Bauer, High dynamic range infrared thermography by pixelwise radiometric self calibration, Infrared Phys. Technol. 53 (2010) 112–119.
[9] S. Chang, Z. Li, Calibration algorithm for cooled mid-infrared systems considering the influences of ambient temperature and integration time, Appl. Opt. 58 (2019) 8118–8125.
[10] C. Songtao, Z. Yaoyu, S. Zhiyuan, L. Min, Method to remove the effect of ambient temperature on radiometric calibration, Appl. Opt. 53 (2014) 6274–6279.
[11] E.C. Fest, Stray light analysis and control, SPIE, 2013.
[12] A. Pravdivtsev, M. Akram, Simulation and assessment of stray light effects in infrared cameras using non-sequential ray tracing, Infrared Phys. Technol. 60 (2013) 306–311.
[13] L. Yang, A. XiaoQiang, W. Qian, Accurate and fast stray radiation calculation based on improved backward ray tracing, Appl. Opt. 52 (2013) B1–B9.
[14] Z. Sun, S. Chang, W. Zhu, Radiometric calibration method for large aperture infrared system with broad dynamic range, Appl. Opt. 54 (2015) 4659–4666.
[15] A. Kattnig, S. Thetas, J. Primot, Ensuring long-term stability of infrared camera absolute calibration, Opt. Express 23 (2015) 18381–18390.
[16] F.E. Nicodemus, Radiometer Calibration for Extended-Source Measurements, J. Opt. Soc. Am. 43 (1953) 547–549.
[17] X. Pang, Y. Yu, Z. Li, Z. Sun, C. Li, G. Yang, Equivalent Calibration Method Based on a Blackbody Baffle Substitution for a Large External Surface-Source Blackbody, Sensors-Basel 22 (2022) 5844.
[18] V. Sapritsky, B. Khlevnoy, V. Khromchenko, B. Lisiansky, S. Mekhontsev, U. Melenevsky, S. Morozova, A. Prokhorov, L. Samoilov, V. Shapoval, Precision blackbody sources for radiometric standards, Appl. Opt. 36 (1997) 5403–5408.
[19] H. Fuyu, S. Xueju, L. Jie, L. Gang, Y. Jiaju, Research on radiometric calibration for super wide-angle staring infrared system, Infrared Phys. Technol. 61 (2013) 9–13.